Magnetic Field Computation in a Physically Large Domain With Thin Metallic Shields

C. Buccella[1], M. Feliziani[1], F. Maradei[2], and G. Manzi[1]

[1]Department of Electrical Engineering, University of L'Aquila, 67040 L'Aquila, Italy
[2]Department of Electrical Engineering, University of Rome La Sapienza, 00184 Rome, Italy

A three-dimensional edge element procedure is presented to analyze the magnetic field around thin shields embedded in a physically large domain. The shield region is eliminated from the computational domain and coupled boundary conditions named impedance network boundary conditions are imposed on the new boundary surfaces to take into account the field discontinuity produced by the eliminated shield. An experimental setup is built and the measured magnetic fields are compared to the results obtained by the proposed procedure.

***Index Terms*—Coupled boundary conditions, edge elements, finite-element method (FEM), impedance network boundary condition (INBC), physically large domain, shielding.**

I. Introduction

SIMULATION of physically large domains in the presence of thin layers of conductive materials is very complicated from a numerical point of view. As example, the characterization of the extremely low frequency (ELF) magnetic field inside a train with alternate current (ac) electrification is quite difficult by traditional three-dimensional (3-D) finite-element method (FEM) codes due to the relevant dimensions of the train (length of 25–30 m for each railway vehicle) with respect to the small dimensions of the aluminum walls of the train carriage with a thickness of 2–3 mm [1]. In the past, many authors have carried out formulations to solve the problem of a conductive thin layer embedded in nonconductive region [2]–[9]. A very efficient approach using the FEM is based on impedance network boundary conditions (INBCs) [2]–[4]. The basic idea of the INBC method is to eliminate from the computational domain the conductive shield by introducing coupled boundary conditions on new boundary surfaces in order to model the penetration of the electric and magnetic fields inside the thin conductive wall. The INBC implementation to the FEM method, i.e., the INBC-FEM method, was carried out for two-dimensional (2-D) eddy current configurations [2] and has been recently applied to solve wave propagation problems in a 3-D domain [4]. Here, the INBC-FEM method is applied to analyze 3-D eddy current regions in presence of thin conductive layers. The method is formulated in terms of the edge element equations and the expressions of the elemental matrices, adequately modified to take into account the field discontinuity produced by the shield, are given. To validate the proposed method, a test application has been built in the laboratory of the University of L'Aquila. This test application has been analyzed by the proposed 3-D INBC-FEM method and by magnetic field measurements.

Digital Object Identifier 10.1109/TMAG.2005.846059

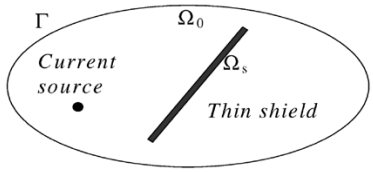

Fig. 1. Computational domain.

II. Mathematical Model

A. Three-Dimensional Formulation of Low-Frequency Shielding Problems

The solution of the 3-D shielding problem, as shown in Fig. 1, requires the analysis of the magnetic field in a nonperfectly conductive region Ω_s, i.e., the shield region, and in the surrounding nonconductive medium Ω_0, i.e., the air region. The time-harmonic magnetic field in $\Omega = \Omega_s + \Omega_0$ is described by the eddy-current equation

$$\nabla \times (\nu \nabla \times \mathbf{A}) = \mathbf{J}_0 + \mathbf{J}_e \tag{1}$$

where $\nu = 1/\mu$, $\mathbf{A}$ is the magnetic vector potential, $\mathbf{J}_0$ is the source current density, and $\mathbf{J}_e$ is the eddy current density which is given by

$$\mathbf{J}_e = -\sigma(\mathrm{j}\omega\mathbf{A} + \nabla\phi) \tag{2}$$

with σ the medium conductivity, $\omega = 2\pi f$ the angular frequency, and ϕ the scalar electric potential.

The introduction of (2) into (1) yields to the following expression:

$$\nabla \times (\nu \nabla \times \mathbf{A}) + \mathrm{j}\omega\sigma\mathbf{A} + \sigma\nabla\phi = \mathbf{J}_0. \tag{3}$$

It should be noted that (3) refers to four unknowns given by the three components of the magnetic vector potential and the scalar electric potential. In order to perform the finite element

solution of the eddy current problem, the following continuity equation should be considered:

$$\nabla \cdot (\mathrm{j}\omega\sigma\mathbf{A} - \sigma\nabla\phi) = 0. \tag{4}$$

By applying the Galerkin method to (3), it yields

$$\int_\Omega \mathbf{w}_\mathrm{k} \cdot \nabla \times (\nu\nabla \times \mathbf{A})\,\mathrm{d}\Omega + \int_\Omega \mathbf{w}_\mathrm{k} \cdot \mathrm{j}\omega\sigma\mathbf{A}\,\mathrm{d}\Omega + \int_\Omega \mathbf{w}_\mathrm{k} \cdot \sigma\nabla\phi\,\mathrm{d}\Omega - \int_\Omega \mathbf{w}_\mathrm{k} \cdot \mathbf{J_0}\,\mathrm{d}\Omega = 0 \tag{5}$$

where $\mathbf{w}_\mathrm{k}$ is the weighting function. Equation (5) can be also written as

$$\int_\Omega (\nabla \times \mathbf{w}_\mathrm{k}) \cdot (\nu\nabla \times \mathbf{A})\,\mathrm{d}\Omega + \int_\Omega \mathbf{w}_\mathrm{k} \cdot \mathrm{j}\omega\sigma\mathbf{A}\,\mathrm{d}\Omega + \int_\Omega \mathbf{w}_\mathrm{k} \cdot \sigma\nabla\phi\,\mathrm{d}\Omega - \int_\Omega \mathbf{w}_\mathrm{k} \cdot \mathbf{J_0}\,\mathrm{d}\Omega + \int_\Gamma \mathbf{w}_\mathrm{k} \cdot (\hat{\mathbf{n}} \times \nu\nabla \times \mathbf{A})\,\mathrm{d}\Gamma = 0 \tag{6}$$

where the last integral is extended to the boundary Γ, and $\hat{\mathbf{n}}$ is the unit vector normal to the boundary surface.

The solution of (3) and (4) can be performed by nodal or vector finite elements and is deeply discussed in [10]. It should be noted that, if inside the computational domain thin conductive panels are present, the eddy current analysis by traditional approaches would lead to the solution of very large problems. To reduce the computational requirements, i.e., computer time and memory storage, the conductive layer Ω_S of thickness d is eliminated from the computational domain, and impedance network boundary conditions INBCs are applied on the conductive panel surfaces Γ_0 and Γ_d, according to the procedure proposed in [2] for 2-D problems using nodal finite elements.

For simplicity, in the following, it is assumed that no further conductive bodies are present in the computational domain. Then, eliminating the thin shield region Ω_S and introducing new boundaries Γ_0 and Γ_d, (6) becomes

$$\int_\Omega (\nabla \times \mathbf{w}_\mathrm{k}) \cdot (\nu\nabla \times \mathbf{A})\,\mathrm{d}\Omega - \int_\Omega \mathbf{w}_\mathrm{k} \cdot \mathbf{J_0}\,\mathrm{d}\Omega + \int_{\Gamma_0} \mathbf{w}_\mathrm{k} \cdot (\hat{\mathbf{n}} \times \nu\nabla \times \mathbf{A}_0)\,\mathrm{d}\Gamma + \int_{\Gamma_\mathrm{d}} \mathbf{w}_\mathrm{k} \cdot (\hat{\mathbf{n}} \times \nu\nabla \times \mathbf{A}_\mathrm{d})\,\mathrm{d}\Gamma + \int_\Gamma \mathbf{w}_\mathrm{k} \cdot (\hat{\mathbf{n}} \times \nu\nabla \times \mathbf{A})\,\mathrm{d}\Gamma = 0. \tag{7}$$

B. Impedance Network Boundary Conditions (INBCs)

Inside the conducting linear region Ω_S of characteristics μ and σ, the penetration of the electric and magnetic field tangential components inside the thin conductive wall can be modeled as a plane wave propagating in a direction normal to the shield surfaces [11]. In this case, the shield layer can be analytically characterized by the following two-port network equations (see Fig. 2):

$$\begin{bmatrix} \hat{\mathbf{n}}_0 \times \mathbf{H}_0 \\ \hat{\mathbf{n}}_\mathrm{d} \times \mathbf{H}_\mathrm{d} \end{bmatrix} = \begin{bmatrix} \mathrm{Y_s} & \mathrm{Y_m} \\ \mathrm{Y_m} & \mathrm{Y_s} \end{bmatrix} \begin{bmatrix} \hat{\mathbf{n}}_0 \times \hat{\mathbf{n}}_0 \times \mathbf{E}_0 \\ \hat{\mathbf{n}}_\mathrm{d} \times \hat{\mathbf{n}}_\mathrm{d} \times \mathbf{E}_\mathrm{d} \end{bmatrix} \tag{8}$$

where $\mathbf{H}_0$ and $\mathbf{H}_\mathrm{d}$ are the magnetic field vectors on the two shield surfaces Γ_0 and Γ_d, respectively, $\mathbf{E}_0$ and $\mathbf{E}_\mathrm{d}$ the corresponding electric field vectors, $\hat{\mathbf{n}}_0$ and $\hat{\mathbf{n}}_\mathrm{d}$ the outward normal unit vectors on the two surfaces Γ_0 and Γ_d, respectively, $\mathrm{Y_s}$ and $\mathrm{Y_m}$ the coefficients of the two-port network admittance matrix given by [11]

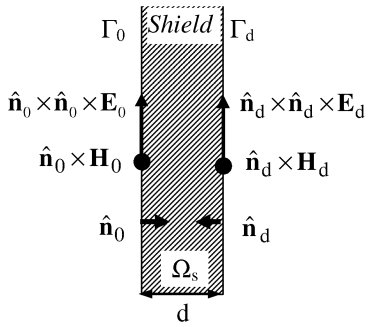

Fig. 2. Tangential field components in the thin shield configuration.

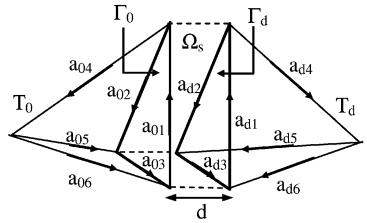

Fig. 3. Configuration of two finite elements adjacent to the shield barrier.

$$\mathrm{Y_s} = \cosh(\gamma\mathrm{d})/[\eta\sinh(\gamma\mathrm{d})] \tag{9a}$$

$$\mathrm{Y_m} = -1/[\eta\sinh(\gamma\mathrm{d}). \tag{9b}$$

Assuming the shield Ω_S as a good conductor, the propagation constant γ and the intrinsic impedance η in (9a) and (9b) can be approximated by

$$\gamma \cong \sqrt{\mathrm{j}\omega\mu\sigma} \tag{10a}$$

$$\eta \cong \sqrt{\mathrm{j}\omega\mu/\sigma}. \tag{10b}$$

To implement INBCs in the FEM formulation (7), the two-port network equations (8) must be expressed in terms of the magnetic vector potential. Assuming in the nonconductive region Ω_0 $\mathbf{E}_0 = \mathrm{j}\omega\mathbf{A}_0$ and $\mathbf{E}_\mathrm{d} = \mathrm{j}\omega\mathbf{A}_\mathrm{d}$, the INBCs (8) can be rewritten as

$$\begin{bmatrix} \hat{\mathbf{n}}_0 \times \nu\nabla \times \mathbf{A}_0 \\ \hat{\mathbf{n}}_\mathrm{d} \times \nu\nabla \times \mathbf{A}_\mathrm{d} \end{bmatrix} = \begin{bmatrix} \mathrm{j}\omega\mathrm{Y_s} & \mathrm{j}\omega\mathrm{Y_m} \\ \mathrm{j}\omega\mathrm{Y_m} & \mathrm{j}\omega\mathrm{Y_s} \end{bmatrix} \begin{bmatrix} \hat{\mathbf{n}}_0 \times \hat{\mathbf{n}}_0 \times \mathbf{A}_0 \\ \hat{\mathbf{n}}_\mathrm{d} \times \hat{\mathbf{n}}_\mathrm{d} \times \mathbf{A}_\mathrm{d} \end{bmatrix}. \tag{11}$$

C. FEM Implementation of INBCs by Edge Elements

The edge element approximation [12] is adopted

$$\mathbf{A} = \sum_{\mathrm{k}=1}^{\mathrm{N^{(e)}}} \mathbf{w}_\mathrm{k} \mathrm{a}_\mathrm{k} \tag{12}$$

where $\mathrm{a_k}$ is the circulation of the magnetic vector potential along the kth edge, $\mathbf{w}_\mathrm{k}$ is the vector trial function, and $\mathrm{N^e}$ is the number of edges per element. Introducing (11) and (12) into (7), the following matrix equation is obtained for the two coupled elements shown in Fig. 3:

$$\begin{bmatrix} [\mathrm{S_0}] - \mathrm{j}\omega\mathrm{Y_s}[\mathrm{D_{00}}] & -\mathrm{j}\omega\mathrm{Y_m}[\mathrm{D_{0d}}] \\ -\mathrm{j}\omega\mathrm{Y_m}[\mathrm{D_{d0}}] & [\mathrm{S_d}] - \mathrm{j}\omega\mathrm{Y_s}[\mathrm{D_{dd}}] \end{bmatrix} \begin{bmatrix} [\mathrm{a_0}] \\ [\mathrm{a_d}] \end{bmatrix} = 0 \tag{13}$$

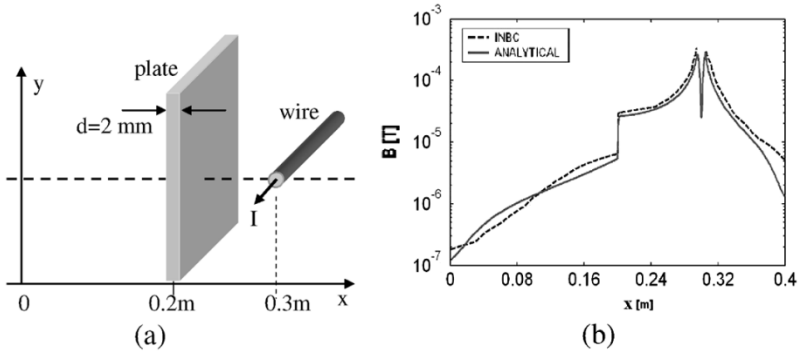

Fig. 4. (a) Wire-plate configuration and (b) magnetic field calculation by the 3-D INBC-FEM method.

where $[a_0]$ and $[a_d]$ are the vectors of the unknown edge values associated with the two tetrahedral elements T_0 and T_d, respectively, and $[S_0]$ and $[S_d]$ are the corresponding stiffness matrices [12]. $[D_{00}]$, $[D_{0d}]$, $[D_{d0}]$, and $[D_{dd}]$ are $N^e \times N^e$ matrices whose kj coefficients (with $k = 1 \ldots N^e, j = 1 \ldots N^e$) are given by

$$D_{00,kj} = \int_{\Gamma_0} \mathbf{w}_k \cdot \mathbf{w}_j \, d\Gamma \quad \text{with } k, j \in T_0 \tag{14a}$$

$$D_{0d,kj} = \int_{\Gamma_0} \mathbf{w}_k \cdot \mathbf{w}_j \, d\Gamma \quad \text{with } k \in T_0 \text{ and } j \in T_d \tag{14b}$$

$$D_{d0,kj} = \int_{\Gamma_d} \mathbf{w}_k \cdot \mathbf{w}_j \, d\Gamma \quad \text{with } k \in T_d \text{ and } j \in T_0 \tag{14c}$$

$$D_{dd,kj} = \int_{\Gamma_d} \mathbf{w}_k \cdot \mathbf{w}_j \, d\Gamma \quad \text{with } k, j \in T_d. \tag{14d}$$

Equation (13) can be seen as the local FEM system for two tetrahedral elements T_0 and T_d placed in the nonconductive region Ω_0 and separated by a shield barrier (see Fig. 3). It should be noted that system (13) is symmetric and of order $2N^e$. The discontinuity of the tangential fields produced by the shield is taken into account by (11), where the admittance matrix coefficients Y_s and Y_m can assume also values different from (9) depending on the kind of shields [11]. For first-order tetrahedral elements, coefficients of (14) are given by

$$\begin{aligned} D_{00,kj} &= 0 \quad \text{if } k \notin \Gamma_0 \text{ or } j \notin \Gamma_0 \\ D_{0d,kj} &= 0 \quad \text{if } k \notin \Gamma_0 \text{ or } j \notin \Gamma_d \\ D_{d0,kj} &= 0 \quad \text{if } k \notin \Gamma_d \text{ or } j \notin \Gamma_0 \\ D_{dd,kj} &= 0 \quad \text{if } k \notin \Gamma_d \text{ or } j \notin \Gamma_d. \end{aligned}$$

Furthermore, it should be pointed out that matrices $[D_{00}] = [D_{dd}]$, $[D_{0d}] = [D_{d0}]$ when the tetrahedral surfaces Γ_0 and Γ_d are identical, i.e., the two adjacent finite elements T_0 and T_d are faced. In this case, if the thickness d of the conductive layer is assumed to be zero $(d = 0)$ only from a geometrical point of view, the two tetrahedra T_0 and T_d have geometrically a common surface $(\Gamma_0 = \Gamma_d)$, but the field quantities in Γ_0 and in Γ_d remain different and coupled by (11) to account the field discontinuity produced by the conductive thin layer [2]–[4]. Finally, when $d = 0$, the generation of the FEM mesh is very advantageous since it is possible to use a normal mesh generator.

III. Applications

As first validation of the proposed method, a simple aluminum wall of 2-mm thickness is excited by a magnetic field produced by a wire current as shown in Fig. 4(a). In the same figure, a comparison between the proposed method and the analytical solution is reported [see Fig. 4(b)].

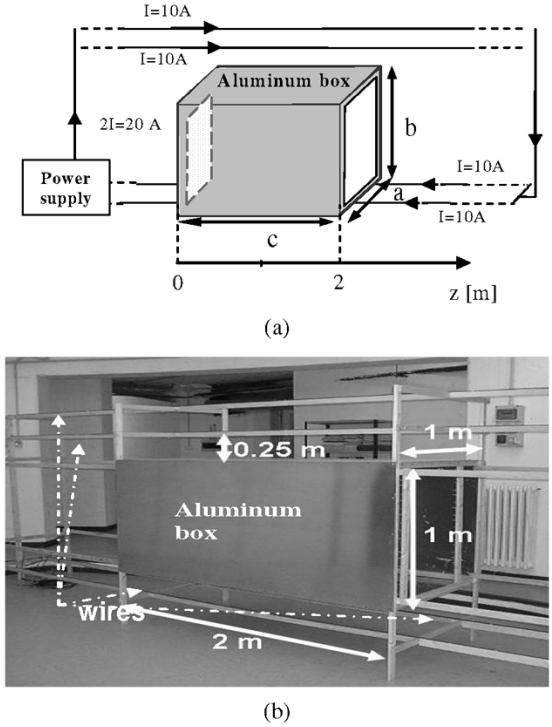

Fig. 5. Experimental setup. (a) Sketch. (b) Photo.

As a second test, an experimental setup has been realized to validate the proposed procedure, by using four aluminum sheets joined together to build a box opened at the two extremity sides. The geometrical dimensions of the aluminum box are: sides $a = 1$ m, $b = 1$ m, $c = 2$ m, and wall thickness $d = 2$ mm. The aluminum box has been excited by the magnetic field generated by four conductors driven, each one, by a current $I = 10$ A at frequency $f = 50$ Hz. Two conductors are placed overlapped above the aluminum box at a distance of 0.25 and 0.5 m from the top of the box, respectively. The other two conductors are both placed at the 0.25 m distance below the box and are separated each other by 0.5 m. The considered experimental setup is shown in Fig. 5.

The electrogeometrical configuration has been simulated by the proposed INBC-FEM procedure. The magnetic flux density B has been also measured at the aperture of the box $(z = 0)$

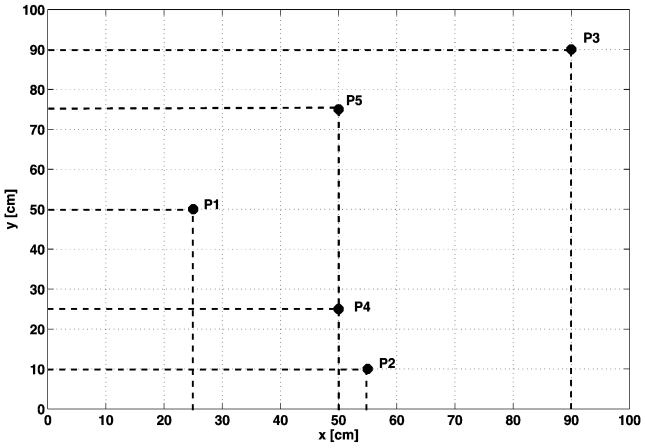

Fig. 6. Map of the measurement points at $z = 0$.

TABLE I
COMPARISON BETWEEN SIMULATED AND MEASURED RESULTS AT FIXED POINTS

Points	Measured B [T]	Simulated by INBC B [T]
P1	$1.10 \cdot 10^{-5}$	$1.20 \cdot 10^{-5}$
P2	$1.75 \cdot 10^{-5}$	$1.85 \cdot 10^{-5}$
P3	$1.55 \cdot 10^{-5}$	$1.60 \cdot 10^{-5}$
P4	$1.30 \cdot 10^{-5}$	$1.50 \cdot 10^{-5}$
P5	$1.25 \cdot 10^{-5}$	$1.35 \cdot 10^{-5}$

by using the Wandel & Goltermann EFA-3 field sensor. The magnetic flux density measured at specific points (P1, P2, P3, P4, and P5 in Fig. 6) are compared with the computed values as reported in Table I.

The results obtained by the proposed method give a good agreement with the measurements results and have been carried out by a significantly reduced computational time.

IV. CONCLUSION

This paper deals with the analysis of the quasistatic magnetic field in presence of thin conductive shields embedded in a nonconductive domain. The method of the INBCs presented in the past by the same authors to analyze 2-D domains by nodal finite elements has been extended to analyze 3-D domains by edge elements. The INBC-FEM method has been validated in real configurations by comparison with the results obtained by magnetic field measurements carried out in a test application device, *ad hoc* built in the laboratory of University of L'Aquila. From the comparison, the INBC-FEM method has revealed to be efficient and accurate to analyze physically large domain with thin conductive layers by the FEM code.

REFERENCES

[1] C. Buccella and M. Feliziani, "Three-dimensional magnetic field computation inside a high speed train with a.c. electrification," presented at the IEEE Int. Symp. EMC, Istanbul, Turkey, May 2003.
[2] M. Feliziani and F. Maradei, "Fast computation of quasistatic magnetic fields around nonperfectly conductive shields," *IEEE Trans. Magn.*, vol. 34, no. 5, pp. 2795–2798, Sep. 1998.
[3] M. Feliziani, F. Maradei, and G. Tribellini, "Field analysis of penetrable conductive shields by the finite-difference time-domain method with impedance network boundary conditions (INBC's)," *IEEE Trans. Electron. Compat.*, vol. 41, no. 4, pp. 307–319, Nov. 1999.
[4] R. A. Ehelers and C. A. R. Metaxas, "3-D FE discontinuos sheet for microwave heating," *IEEE Trans. Microwave Theory Tech.*, vol. 51, no. 3, pp. 718–726, Mar. 2003.
[5] P. A. Tirkas and K. R. Demarest, "Modeling of thin dielectric structures using the finite-difference time-domain technique," *IEEE Trans. Antennas Propagat.*, vol. 39, no. 9, pp. 1338–1344, Sep. 1991.
[6] E. H. Newman, "A sheet impedance approximation for electrically thick material shields," *IEEE Trans. Antennas Propagat.*, vol. 50, no. 4, pp. 435–443, Apr. 2002.
[7] H. Igarashi, A. Kost, and T. Honma, "A three dimensional analysis of magnetic fields around a thin magnetic conductive layer using vector potential," *IEEE Trans. Magn.*, vol. 34, no. 5, pp. 2539–2542, Sep. 1998.
[8] D. Rodger, P. J. Leonard, and H. C. Lai, "Surface elements for modeling 3D fields around thin iron sheets," *IEEE Trans. Magn.*, vol. 29, no. 2, pp. 1483–1486, Mar. 1993.
[9] O. Biro, I. Bardi, K. Preis, W. Renhart, and K. R. Richter, "A finite element formulation for eddy current carrying ferromagnetic thin sheets," *IEEE Trans. Magn.*, vol. 33, no. 2, pp. 1173–1178, Mar. 1997.
[10] S. R. H. Hoole, Ed., *Finite Elements, Electromagnetics, and Design*. Amsterdam, The Netherlands: Elsevier, 1995.
[11] R. B. Schulz, V. C. Plantz, and D. R. Brush, "Shielding theory and practice," *IEEE Trans. Electromagn. Compat.*, vol. 30, no. 3, pp. 187–201, Aug. 1988.
[12] J. Jin, *The Finite Element Methods in Electromagnetics*. New York: Wiley, 1993.

Manuscript received June 6, 2004.